Pancreatology xxx (xxxx) xxx

Contents lists available at ScienceDirect

Pancreatology

journal homepage: www.elsevier.com/locate/pan

Inhibition of mouse trypsin isoforms by SPINK1 and effect of human pancreatitis-associated mutations

Nataly C. Morales Granda [a, b], Vanda Toldi [a], Mário Miczi [a], Meriam Lassoued [a], András Szabó [a, *]

[a] Department of Biochemistry and Molecular Biology, Faculty of Medicine, University of Debrecen, Debrecen, Hungary
[b] Doctoral School of Molecular, Cell and Immune Biology, University of Debrecen, Debrecen, Hungary

ARTICLE INFO

Article history:
Received 4 April 2023
Received in revised form
26 April 2023
Accepted 28 April 2023
Available online xxx

Keywords:
Trypsin
Inhibition
Mutation
Chronic pancreatitis
Inflammation

ABSTRACT

Serine protease inhibitor Kazal type 1 (SPINK1) is a trypsin-selective inhibitor protein secreted by the exocrine pancreas. Loss-of-function SPINK1 mutations predispose to chronic pancreatitis through either reduced expression, secretion, or impaired trypsin inhibition. In this study, we aimed to characterize the inhibitory activity of mouse SPINK1 against cationic (T7) and anionic (T8, T9, T20) mouse trypsin isoforms. Kinetic measurements with a peptide substrate, and digestion experiments with β-casein indicated that the catalytic activity of all mouse trypsins is comparable. Human SPINK1 and its mouse ortholog inhibited mouse trypsins with comparable efficiency (K_D range 0.7−2.2 pM), with the sole exception of T7 trypsin, which was inhibited less effectively by the human inhibitor (K_D 21.9 pM). Characterization of four chronic pancreatitis-associated human SPINK1 mutations in the context of the mouse inhibitor revealed that the reactive-loop mutations R42N (human K41N) and I43M (human I42M) impaired SPINK1 binding to trypsin (K_D 60 nM and 47.5 pM, respectively), whereas mutations D35S (human N34S) and A56S (human P55S) had no impact on trypsin inhibition. Our results confirmed that high-affinity trypsin inhibition by SPINK1 is conserved in the mouse, and the functional consequences of human pancreatitis-associated SPINK1 mutations can be replicated in the mouse inhibitor.

1. Introduction

The human exocrine pancreas expresses and secretes two major trypsins as inactive precursors, also known as zymogens. These proteases were named as cationic trypsinogen and anionic trypsinogen based on their relative electrophoretic mobility in native gels [1]. Trypsinogens can be proteolytically activated by the brush border enzyme enteropeptidase upon reaching the duodenum. In addition, trypsinogens are capable of autoactivation in a bimolecular reaction when trypsin activates trypsinogen. Trypsins also proteolytically activate several other pancreatic digestive proteases; such as chymotrypsinogen, proelastase and procarboxypeptidase. Premature intrapancreatic trypsinogen activation can lead to the development of chronic pancreatitis, an irreversible inflammatory disorder of the pancreas [2,3]. Therefore, trypsinogen activation is strictly regulated by the trypsin specific serine protease inhibitor Kazal type 1 (SPINK1) protein, also secreted by the exocrine pancreas [4]. Human SPINK1 is a tight-binding canonical inhibitor, which contributes about 2−13% of trypsinogen content [3]. Despite its low amount, SPINK1 efficiently delays trypsinogen activation, and prevents the onset of pancreatitis. Loss-of-function mutations in SPINK1; including promoter variants, splice variants, nucleotide insertion or deletions, start-loss variants, signal peptide variants that reduce secretion, and missense variants were associated with an increased risk for the development of chronic pancreatitis [3,5]. Missense SPINK1 mutations exert their pathological effect through reduced secretion of the inhibitor or impaired trypsin inhibition [3,5]. Apart from that, SPINK1 was described as a cell growth and survival factor that promotes cell proliferation and metastasis in a variety of cancers [6].

Mice carrying trypsinogen mutations resulting in spontaneous intrapancreatic protease activation have been successfully developed to model chronic pancreatitis [7]. The mouse pancreas secretes four trypsinogens, which are known as T7, T8, T9 and T20 [8]. Among mouse trypsinogens, T7 has a cationic character, whereas

* Corresponding author. Department of Biochemistry and Molecular Biology, Faculty of Medicine, University of Debrecen, Debrecen, Egyetem tér 1, Life Science Building 3.503, H-4032, Hungary.
E-mail address: andrasszabo@med.unideb.hu (A. Szabó).

https://doi.org/10.1016/j.pan.2023.04.043

T8, T9 and T20 are all anionic trypsinogens. Each of the mouse trypsinogens contribute about 30% of total trypsinogen, with the exception of T20, which provides only about 10% of it [8]. Trypsinogens T8, T9 and T20 share more than 90% sequence identity on the amino acid level, whereas trypsinogen T7 shares only about 76–78% sequence identity with the other mouse trypsinogens. The mouse pancreas also secretes a trypsin inhibitor protein encoded by the *Spink1* gene (legacy name *Spink3*), which is orthologous to human SPINK1. The mouse SPINK1 inhibitor shares about 63% sequence identity to its human counterpart.

Several studies reported that homozygous deficiency of mouse SPINK1 results in degenerative development of the pancreas, leading to the death of the animals within two weeks after birth [9,10]. The lethal phenotype could be rescued by crossing the SPINK1 deficient mice with transgenic mice expressing rat or human SPINK1 [10,11]. Additionally, the pancreas-specific expression of rat SPINK1 in mice reduced the severity of induced acute and chronic pancreatitis [12–14]. Numerous human SPINK1 mutations identified in chronic pancreatitis reduce the expression and secretion of the inhibitor. A recent study reported that the common c.194+2T>C splice site SPINK1 mutation in heterozygous form resulted in spontaneous development of chronic pancreatitis in mice [15]. However, mouse models expressing chronic pancreatitis-associated missense SPINK1 variants have not been developed so far. To achieve this, here we performed a comprehensive *in vitro* study to characterize the activity of mouse trypsins and the binding of mouse SPINK1 to trypsins. We also assessed the effect of four readily secreted SPINK1 variants associated with chronic pancreatitis on the inhibition of mouse trypsins.

2. Methods

2.1. Nomenclature

Amino acid sequence numbering of SPINK1 starts with the initiator methionine of the primary translation product. Note that the N-terminus of mouse SPINK1 (legacy name SPINK3) carries an additional amino acid, therefore, the amino acid numbering is shifted by one compared to human SPINK1.

2.2. Expression plasmids

The pTrapT7 plasmid carrying the coding DNA of mouse trypsinogens were reported previously [8]. The mammalian expression plasmid pcDNA3.1(−) containing human SPINK1-10His-minigene-1 was described earlier [5]. DNA fragments corresponding to mouse SPINK1 (NCBI Reference Sequence: NM_009258.5) exon-1 and exons 2–4 were custom synthesized by GeneScript and cloned into the human SPINK1-10His-minigene-1 expression plasmid using XhoI-XcmI and EcoRI-HindIII restriction sites, respectively. Mutations were generated by overlap extension PCR mutagenesis. The sequence of all plasmid DNA constructs were verified by capillary sequencing.

2.3. Expression and purification of SPINK1

HEK 293T cells were grown in T75 tissue culture flasks in high-glucose DMEM supplemented with 10% fetal bovine serum, 4 mM glutamine, 50 U/ml penicillin and 50 μg/ml streptomycin at 37 °C in a cell culture incubator. At 70–90% confluence, the cells were transiently transfected with 10 μg human or mouse SPINK1-10His-minigene-1 plasmid DNA following a recently described protocol [5]. The standard cell culture medium was removed and SPINK1 protein secretion was achieved in Opti-MEM medium, supplemented with penicillin and streptomycin in a tissue culture incubator. The conditioned medium was harvested after 48 h, followed by an additional 48 h expression cycle. For a typical SPINK1 expression, eight T75 flasks were used. Conditioned media containing SPINK1 were pooled and SPINK1 was purified with a 5 mL HisPur Ni-NTA Chromatography Cartridge (Thermo Scientific) attached to an FPLC system based on a previous protocol [5]. SPINK1 was eluted with 50 mM NaH_2PO_4, 300 mM NaCl, 250 mM imidazole (pH 8.0) buffer. Fractions containing pure SPINK1 were pooled and dialyzed against 20 mM Tris-HCl (pH 8.0) buffer. SPINK1 concentration was determined with titration against trypsin preparations used for the binding experiments with the exception of the defective R42N mouse SPINK1 variant, which was determined by SDS-PAGE, Coomassie Blue staining, and densitometry, using an active site–titrated SPINK1 standard.

2.4. Expression and purification of trypsinogen

Mouse trypsinogens were expressed in *E. coli* BL21(DE3) cells, isolated from inclusion bodies and refolded *in vitro* as previously described [8]. Trypsinogens were purified with an ecotin affinity column attached to an FPLC system. The ecotin column was equilibrated with washing buffer (20 mM Tris-HCl (pH 8.0) and 0.2 M NaCl buffer). Trypsinogen sample was loaded onto the column, protein contaminants were removed from the column with washing buffer and pure trypsinogen was eluted with 50 mM HCl and stored in aliquots at −20 °C. If trypsin was needed, trypsinogen was activated with human recombinant enteropeptidase (Bio-Techne) in 0.1 M Tris-HCl (pH 8.0) and 1 mM $CaCl_2$ buffer. Ecotin inhibited mouse trypsins with apparent dissociation constant (K_D) values in the low picomolar range (Supplementary Table 1), therefore trypsin concentrations were determined by active site titration against ecotin.

2.5. Analysis of β-casein digestion by SDS-PAGE

β-casein at 0.2 mg/ml was incubated with 10 nM trypsin in 0.1 M Tris-HCl (pH 8.0) buffer supplemented with 1 mM $CaCl_2$ and 0.05% Tween 20 at 37 °C. At given time points 0.1 ml aliquots were withdrawn and the reaction was terminated by adding 10% final trichloroacetic acid. Precipitated proteins were centrifuged at 16,000 g for 10 min and re-dissolved in 15 μl Laemmli buffer containing 0.1 M dithiothreitol, heat-denatured for 5 min at 90 °C and electrophoresed by 15% SDS-PAGE. Protein bands in the gels were stained with Coomassie Brilliant Blue R-250. Gel images were taken by the Azure 600 Imaging System (Azure Biosystems). Loss of the intact β-casein band was quantified by densitometry using Quantity One software 4.6.6 (Bio-Rad).

2.6. Enzyme kinetic measurements

Enzyme kinetic parameters of mouse trypsins were determined using Suc-Ala-Ala-Pro-Lys-p-nitroanilide chromogenic substrate. Substrate concentrations varied between 0.025 mM and 0.8 mM in 0.1 M Tris-HCl (pH 8.0), 1 mM $CaCl_2$ and 0.05% Tween 20 buffer. Measurements were initiated by the addition of 25 nM final trypsin. The release of the yellow p-nitroaniline was followed for 1 min at 405 nm using a BioTek Synergy H1 multimode microplate reader, and the rate of substrate cleavage was determined from the linear portions of the curves. *K*m and V_{max} values were calculated from hyperbolic fits to plots of velocity versus substrate concentration.

2.7. Inhibitor binding assays

Binding of SPINK1 to trypsins were assessed by measuring the apparent dissociation constant (K_D) values as reported previously

[5]. Trypsin in a fixed concentration was incubated with increasing concentrations of inhibitor in 0.1 M Tris–HCl (pH 8.0), 150 mM NaCl, 1 mM $CaCl_2$, and 0.05% Tween 20 buffer. When reaching equilibrium, trypsin activity was measured by the addition of 0.15 mM final concentration of Z-Gly-Pro-Arg-AMC fluorogenic substrate at 380 nm excitation and 460 nm emission wavelength with a fluorescent plate reader. Apparent K_D values were calculated by plotting the free trypsin concentration as a function of the total inhibitor concentration and fitting the data points to the following equation: y = E − (E + x + K-sqrt((E + x + K)^2 − 4Ex))/2, where the independent variable x represents the total inhibitor concentration, the dependent variable y is the free protease concentration in equilibrium, K is K_D, and E designates the total protease concentration. Association rate constant (k_{on}) and dissociation rate constant (k_{off}) measurements were carried out as described earlier [5], with the exception of the R42N SPINK1, in which case binding to trypsin was monitored with bio-layer interferometry. An Anti-penta-His biosensor was attached to the BLItz instrument (ForteBio). SPINK1-10His and T7 trypsin were diluted with Tris-buffered saline (pH 7.5) containing 0.05% Tween 20 to 1 μM and 50 nM final concentrations, respectively. All steps were carried out with vigorous agitation at 2200 rpm at 22 °C. SPINK1-10His protein was immobilized by dipping the biosensor tip in the inhibitor solution until reaching equilibrium. The association and the dissociation measurements were performed by submerging the biosensor tip in trypsin solution for 2 min and in Tris-buffered saline (pH 7.5) containing 0.05% Tween 20 for additional 3 min, respectively. A baseline without trypsin was also recorded and subtracted from the results.

3. Results

3.1. Characterization of mouse trypsin isoforms

Four trypsins expressed and secreted by the mouse pancreas are highly homologous proteases. To functionally characterize and compare the specificity of mouse trypsins, we measured their enzyme kinetic parameters using a short chromogenic peptide substrate (Table 1). The rate constant (k_{cat}) values for trypsins T7, T9, T20 were about 28.2–32.5 s^{-1}, whereas the k_{cat} value for T8 was somewhat lower (21.9 s^{-1}). The Michaelis constant (K_m) values for T7 and T9 were about 146 μM and 140 μM, whereas the K_m values for T9 and T20 were somewhat lower at 99.9 μM and 74.6 μM, respectively. Based on the enzyme kinetic parameters, the calculated specificity constant (k_{cat}/K_m) values of mouse trypsins exhibited only a two-fold difference in the range of 2.0 × 10^5 and 4.4 × 10^5 M^{-1} s^{-1}.

As natural protein substrates are more relevant in biological systems to study the efficacy of pancreatic trypsins, we compared the activity of mouse trypsins by following the degradation of β-casein over time by protein gel electrophoresis (Fig. 1). Mouse trypsin T7 digested β-casein effectively, and even higher degradation rates were detected for trypsins T8, T9 and T20. Interestingly, the banding pattern of digested β-casein by T7 was similar to that produced by T20, but differed from the cleavage patterns generated by T8 and T9. The cleavage pattern of β-casein with trypsin T8 resembled that of T9.

Table 1
Enzyme kinetic parameters of mouse trypsins. Measurements were performed using Suc-Ala-Ala-Pro-Lys-p-nitroanilide substrate as described in Methods. Kinetic parameters were determined using hyperbolic functions fitted to the average of three measurements.

	T7	T8	T9	T20
k_{cat} (s^{-1})	28.7 ± 0.8	21.9 ± 0.6	29.9 ± 1.4	32.5 ± 2.5
K_m (μM)	146 ± 12	99.9 ± 9.7	140 ± 20	74.6 ± 17.6
k_{cat}/K_m (M^{-1} s^{-1})	2.0 × 10^5	2.2 × 10^5	2.1 × 10^5	4.4 × 10^5

3.2. Binding of human and mouse SPINK1 to mouse trypsin isoforms

Canonical protease inhibitors bind to the active site of protease targets through an exposed surface loop called reactive loop. Human SPINK1 is a tight-binding canonical inhibitor of human cationic and anionic trypsins. To study how human SPINK1 inhibits mouse trypsins, we measured the apparent dissociation constant values (K_D) in equilibrium (Fig. 2). We found that human SPINK1 inhibited mouse trypsin T7 with a K_D value of 21.9 pM, in contrast, an order-of-magnitude lower K_D values (1.5–2.2 pM) were detected against trypsins T8, T9 and T20. We also determined the K_D values of the orthologous mouse SPINK1 against mouse trypsins. Interestingly, mouse SPINK1 strongly inhibited T7 and all other mouse trypsins, indicated by the low K_D values in the range of 0.7–1.9 pM.

3.3. Binding of mouse SPINK1 variants to mouse trypsins

Reduced inhibitory activity of human SPINK1 against trypsin predispose to chronic pancreatitis. We expressed and purified the D35S (human N34S), R42N (human K41N), I43 M (human I42M) and A56S (human P55S) readily secreted mouse SPINK1 variants, originally identified in patients with chronic pancreatitis and sometimes in healthy subjects. The position of the mutations in the primary structure of SPINK1 is shown in Fig. 3. First, we measured the apparent equilibrium K_D values of the mouse SPINK1 variants against T7 trypsin to compare their binding to the wild-type inhibitor (Fig. 4 and Table 2). Trypsin inhibition by the D35S SPINK1 variant was comparable to that of the wild-type. The A56S variant possessed around 3-fold weaker binding to T7, whereas the R42N and I43M reactive loop variants had about 37,000-fold and 30-fold weaker binding to T7 than wild-type SPINK1, respectively. Consistent with this notion, the D35S and A56S variants were highly effective inhibitors of T8, T9, and T20 trypsins, while the reactive loop variants inhibited trypsins by several orders of magnitude weaker (Fig. 5 and Table 2).

Alternatively, mouse SPINK1 binding to trypsin can be characterized by measuring the rate constants of the inhibitor, as detailed in Fig. 6 and Table 2. The association rate constant (k_{on}) values of wild-type mouse SPINK1 were in the range of 7.1 × 10^6 and 8.2 × 10^6 M^{-1} s^{-1} against T7, T8 and T9, while a somewhat increased k_{on} value (20.3 × 10^6 M^{-1} s^{-1}) was determined against T20 (Fig. 6A). Comparable k_{on} values were detected for D35S, I43M and A56S mouse SPINK1 variants against mouse trypsins. The dissociation rate constant (k_{off}) values of wild-type mouse SPINK1 were between 0.6 × 10^{-5} and 1.2 × 10^{-5} s^{-1} against the mouse trypsins, and the k_{off} values for D35S and A56S variants remained below 5.3 × 10^{-5} s^{-1} (Fig. 6B). In contrast to wild-type mouse SPINK1, the k_{off} values of the I43M variant against mouse trypsins were increased by at least an order-of-magnitude. Overall, the elevated k_{off} value and the relatively unchanged k_{on} values of the I43M variant contributed to the increased K_D values and decreased trypsin inhibition. Due to technical difficulties, we were unable to determine the rate constants of the R42N mouse SPINK1 variant with trypsin activity based methods, therefore we compared association and dissociation kinetics of the wild-type SPINK1 and R42N variant using biolayer interferometry (Fig. 6C). The measurements indicated that the highly elevated K_D value of the R42 N variant is due to impaired association with trypsin.

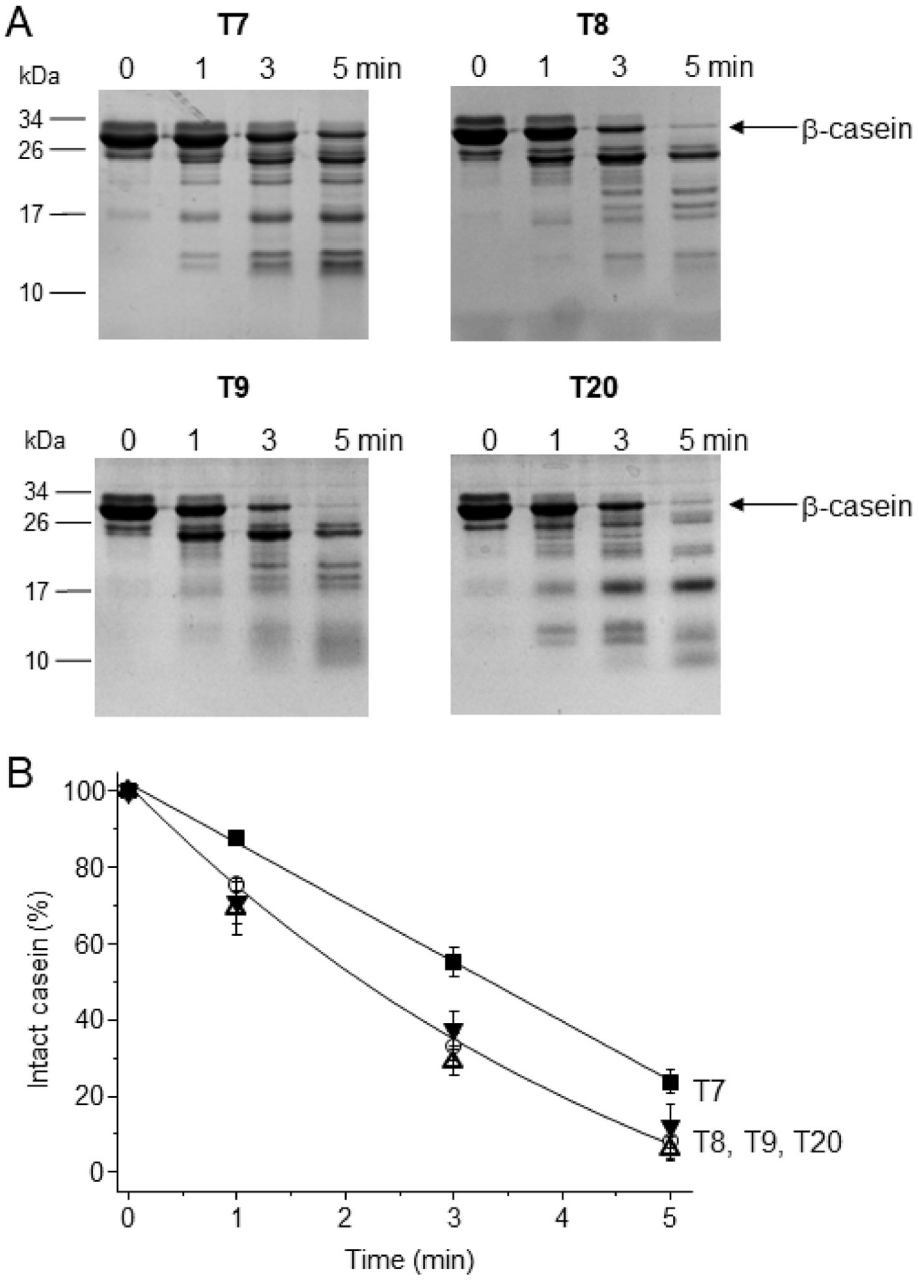

Fig. 1. Digestion of β-casein by mouse trypsins. Representative gel images (A) and densitometric evaluations (B) are shown. Experiments were carried out as described in Methods. Mean ± SD of three experiments are shown.

3.4. Auto-activation of T7 trypsinogen in the presence of wild-type mouse SPINK1 and inhibitory loop variants

The physiological role of SPINK1 is to prevent premature intrapancreatic protease activation by delaying trypsinogen auto-activation. We studied the effect of wild-type mouse SPINK1, and the R42N and I43M variants on the auto-activation of T7 trypsinogen (Fig. 7). Under the experimental conditions, the wild-type mouse SPINK1 delayed trypsinogen activation by about 40 min. The inhibitory effect of I43M variant was comparable to the wild-type inhibitor, while R42N variant had no delaying effect on trypsinogen auto-activation.

4. Discussion

Despite the increasing number of articles on mouse trypsins, the substrate specificity and kinetic parameters of these proteases remained mostly uncharacterized. In this study, first we compared the kinetic parameters of mouse T7, T8, T9 and T20 trypsins using a short chromogenic peptide substrate with Lys at the cleavage site. We found that the primary substrate specificity of trypsins are relatively unchanged, only T20 possessed a slightly higher specificity constant value. Recently published kinetic parameters of mouse trypsins on another short peptide substrate with Arg at the cleavage site confirmed that T20 is the most efficient one among mouse trypsins [16]. Protein substrates are more relevant to compare the activity of trypsins. Therefore, we determined the cleavage rates of mouse trypsins using the dietary β-casein protein

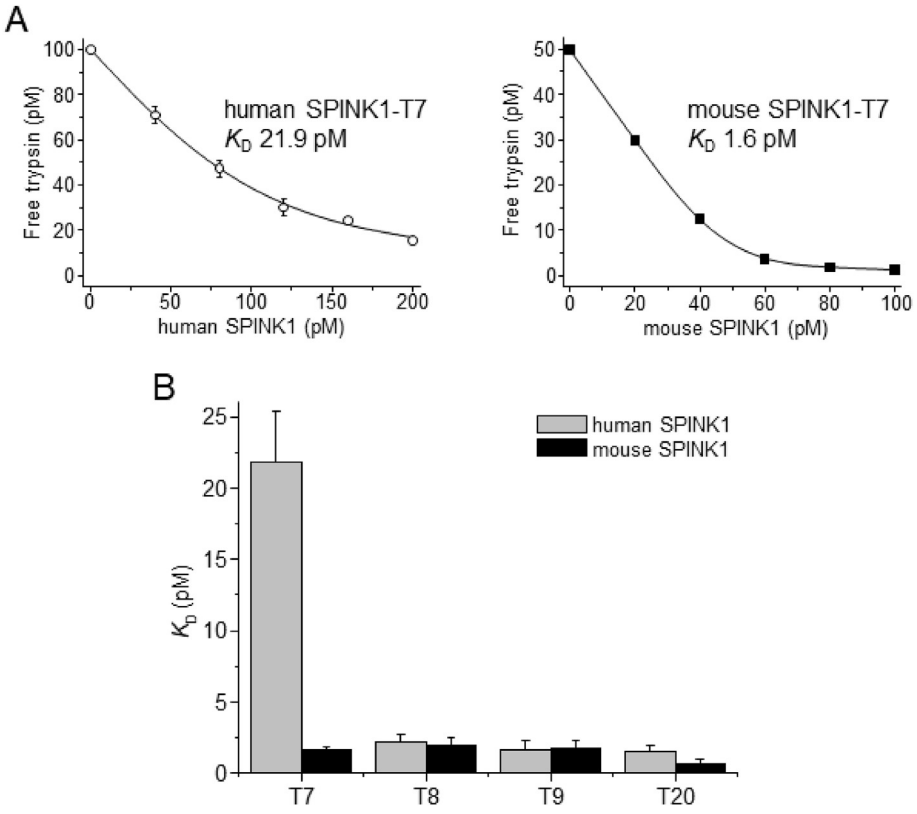

Fig. 2. Inhibition of mouse trypsins by human and mouse SPINK1. Representative binding experiments of human SPINK1 and mouse SPINK1 to mouse T7 trypsin was characterized by determining the dissociation constant (K_D) values in equilibrium (A). Equilibrium K_D values of human and mouse SPINK1 against mouse trypsins (B). Measurements were carried out as described in Methods. Data point represents the mean ± SD of three or four experiments.

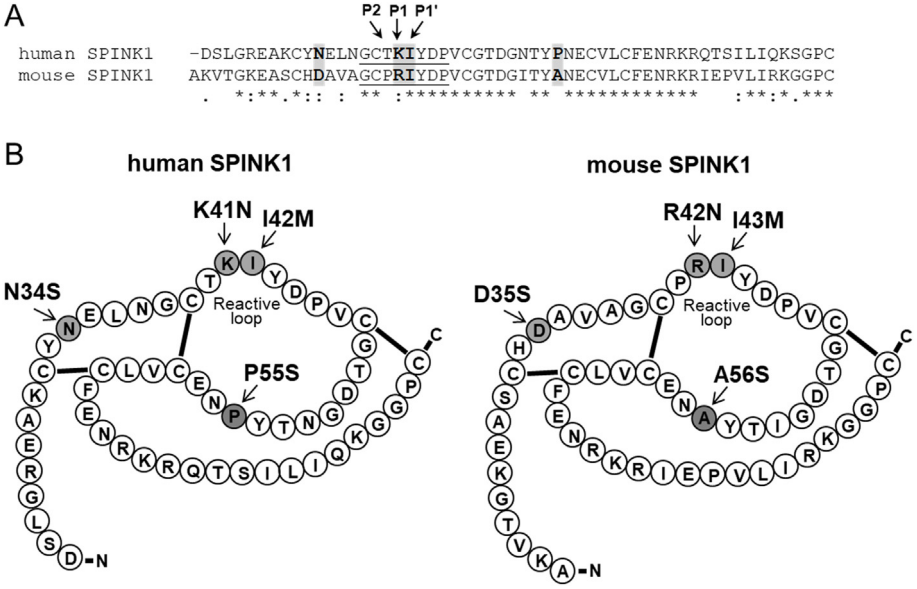

Fig. 3. Sequence comparison of human and mouse SPINK1 inhibitors. Amino acid sequence alignment of human SPINK1 and mouse SPINK1 indicating the mutation sites of interest in grey (A). The sequence of the reactive loop is underlined, where P1–P1' (Schechter-Berger numbering) indicates the scissile peptide bond. Schematic structure of human versus mouse SPINK1 showing the investigated mutation sites (B).

as substrate. The results indicated comparable cleavage rates by all mouse trypsins. Interestingly, trypsin T7 generated similar β-casein fragments to T20, but differed from the cleavage pattern achieved by T8 and T9. Although not thoroughly investigated, these results suggested that there are certain alterations in the substrate specificity of mouse trypsins.

SPINK1 is a trypsin-specific inhibitor protein, which binds to the active site of the protease in a substrate-like manner [17]. Human

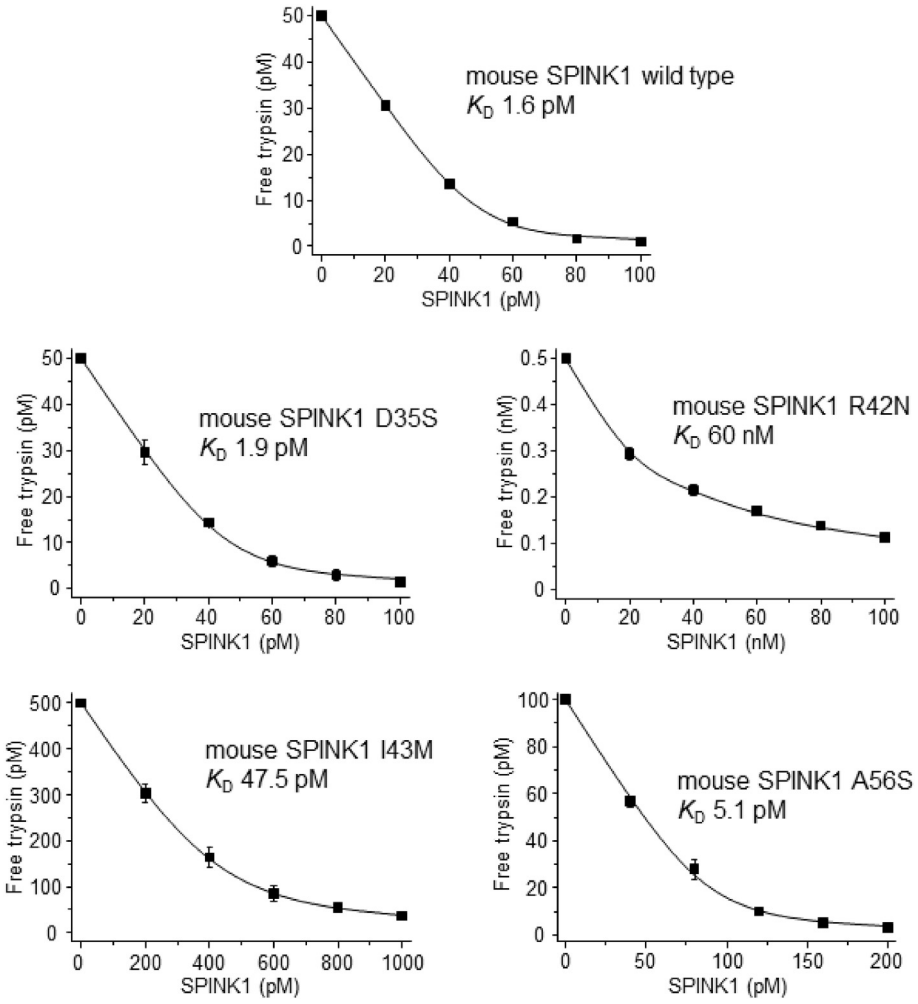

Fig. 4. Inhibition of T7 trypsin by mouse SPINK1 wild type and variants. Binding of SPINK1 to trypsin was characterized by measuring the dissociation equilibrium constant (K_D) values in equilibrium as described in Methods. Data from three experiments were fitted globally. Data points represent mean ± SD. Symbol size may be larger than the error bars.

and mouse SPINK1 are highly homologous canonical inhibitors that differ only at the P1 (Lys vs Arg) and P2 (Thr vs Pro) positions (Schechter-Berger numbering) in the reactive loop (see Fig. 3A). Phage display selection of SPINK1 against trypsin suggested that P1 Lys or Arg is required to ensure inhibitor binding and P2 Thr or Pro is essential to maintain structural stability of the inhibitor [18]. Here we compared the binding of human SPINK1 and mouse SPINK1 to all four mouse trypsins. K_D values in the low picomolar range indicated that both human SPINK1 and mouse SPINK1 bind to mouse trypsins with high affinity, effectively inhibiting them. The only notable difference between human and mouse SPINK1 was observed when assayed against trypsin T7. In a previous comprehensive study, we found equally strong binding of human SPINK1 to recombinant non-sulfated human cationic and anionic trypsins [5]. *In vivo,* human trypsins are posttranslationally sulfated near the active site, which somewhat decreases human SPINK1 binding affinity [19]. As rodent trypsins are not sulfated, we assume that trypsin inhibition in the mouse pancreas is even more effective.

Loss-of-function mutations in human SPINK1 are associated with the inflammatory disorder chronic pancreatitis [3]. To date, about 20 missense SPINK1 mutations were identified in subjects diagnosed with chronic pancreatitis. In this study, the functional consequences of four mutations were investigated in the mouse orthologous inhibitor. Mutations N34S and P55S located in the inhibitor scaffold are common in healthy human populations [5]. Genetic analyses revealed that the N34S mutation is strongly associated with chronic pancreatitis [20,21]. However, several functional studies demonstrated that the mutation has no effect on either human SPINK1 secretion or inhibitory activity as compared to the wild-type inhibitor [5,22–28]. Most likely, the N34S mutation is inherited together with another mutation located in the 5′ region upstream of the gene and predispose to chronic pancreatitis by diminishing SPINK1 mRNA expression [29]. Genetic studies indicated that the P55S mutation is clinically insignificant, as it was identified in both subjects with chronic pancreatitis and healthy individuals with similar frequencies [5,21]. Functional characterizations demonstrated that the mutation has no effect on secretion and it only slightly weakens the inhibition of human trypsins by SPINK1 [5,24,25]. The Asn34 and Pro55 are not evolutionarily conserved amino acid residues. Mutations D35S and A56S are the mouse equivalents of the N34S and P55S human SPINK1 mutations. Both the D35S and A56S mouse SPINK1 variants are readily secreted. Similarly to the wild-type inhibitor, the D35S mouse SPINK1 effectively and uniformly inhibited all mouse trypsins. Consistent with studies on human SPINK1, the A56S mouse SPINK1 variant exhibited comparable binding to mouse trypsins T8, T9 and T20 and an inconsequentially weaker binding to T7.

Table 2
Equilibrium dissociation constant ($K_{D(eq)}$) values and association (k_{on}) and dissociation (k_{off}) rate constants determined for mouse SPINK1 wild type and variant against mouse tryspins. Measurements of at least three experiments are shown. Measurements were carried out as described in Methods. Alternatively, K_D values were calculated by dividing k_{off} by k_{on}. ND – not determined.

mouse SPINK1	T7	T8	T9	T20
wild type				
k_{on} (x10^6 $M^{-1}s^{-1}$)	7.1 ± 0.5	7.2 ± 0.4	8.2 ± 0.4	20.3 ± 0.6
k_{off} (x10^{-5} s^{-1})	1.2 ± 0.2	0.7 ± 0.1	0.7 ± 0.3	0.6 ± 0.05
$K_{D(calc)}$ (pM)	1.7	1.0	0.9	0.3
$K_{D(eq)}$ (pM)	1.6 ± 0.2	1.9 ± 0.6	1.8 ± 0.6	0.7 ± 0.3
D35S				
k_{on} (x10^6 $M^{-1}s^{-1}$)	8.2 ± 0.5	8.3 ± 0.3	5.2 ± 0.3	20.8 ± 0.6
k_{off} (x10^{-5} s^{-1})	3.8 ± 0.9	1.1 ± 0.1	1.7 ± 0.4	0.07 ± 0.02
$K_{D(calc)}$ (pM)	4.6	1.3	3.3	0.03
$K_{D(eq)}$ (pM)	1.9 ± 0.7	2.9 ± 0.4	4.0 ± 0.8	0.3 ± 0.1
R42N				
k_{on} (x10^6 $M^{-1}s^{-1}$)	ND	ND	ND	ND
k_{off} (x10^{-5} s^{-1})	ND	ND	ND	ND
$K_{D(calc)}$ (pM)	ND	ND	ND	ND
$K_{D(eq)}$ (μM)	0.060 ± 0.001	0.18 ± 0.01	1.06 ± 0.16	1.13 ± 0.13
I43M				
k_{on} (x10^6 $M^{-1}s^{-1}$)	6.6 ± 0.5	11.1 ± 0.3	6.8 ± 0.5	22.8 ± 0.5
k_{off} (x10^{-5} s^{-1})	15.1 ± 2.1	21.2 ± 0.8	32.3 ± 5.6	10.4 ± 1.9
$K_{D(calc)}$ (pM)	22.9	19.1	47.5	4.6
$K_{D(eq)}$ (pM)	47.5 ± 3.5	170 ± 14	338 ± 56	35.3 ± 5.7
A56S				
k_{on} (x10^6 $M^{-1}s^{-1}$)	5.3 ± 0.4	13.6 ± 0.4	11.5 ± 1.2	22.6 ± 0.5
k_{off} (x10^{-5} s^{-1})	5.3 ± 2.0	0.2 ± 0.04	0.2 ± 0.07	0.7 ± 0.1
$K_{D(calc)}$ (pM)	10.0	0.1	0.2	0.3
$K_{D(eq)}$ (pM)	5.1 ± 0.7	1.6 ± 0.3	2.4 ± 0.3	1.4 ± 0.3

Both K41N and I42M are uncommon human SPINK1 mutations described only once in a case of early-onset recurrent acute pancreatitis [30,31]. The patient carrying the I42M mutation also carried a chymotrypsin C mutation and a cystic fibrosis transmembrane conductance regulator (CFTR) protein mutation, whereas the patient carrying the K41N mutation also carried a chronic pancreatitis-associated CFTR mutation. In agreement with a previous functional study [5], the corresponding R42N and I43M mouse SPINK1 variants are readily secreted in transfected mammalian cells. Both mutations are situated in the reactive loop of SPINK1 and markedly affect trypsin inhibition. The R42N variant bound 4 to 6 orders-of-magnitude weaker to mouse trypsin than wild-type mouse SPINK1, whereas the I43M variant caused an order-of-magnitude weaker mouse trypsin inhibition than the wild-type inhibitor. The determination of the rate constant values indicated that the I43M mouse SPINK1 variant exhibited a weaker trypsin inhibition due to increased dissociation rate and relatively unchanged association kinetic. Our measurements on the R42N variant suggested that the defective association of mouse SPINK1 resulted in reduced trypsin inhibition.

The human exocrine pancreas expresses much lower amount of SPINK1 than trypsin [3]. SPINK1 is a temporary inhibitor as it is inactivated and degraded by trypsin over time [5,32]. The role of SPINK1 is to delay trypsinogen auto-activation, thereby, protecting the pancreas against auto-digestion and the development of inflammation [3]. To compare the effect of mouse SPINK1 variants on trypsinogen auto-activation, we activated mouse T7 trypsinogen in the absence and presence of mouse SPINK1 and measured trypsin activity. In agreement with the binding studies, the R42N mouse SPINK1 variant did not inhibit trypsinogen activation. In contrast, the inhibition of trypsinogen activation by the I43M mouse SPINK1 variant was closely identical to that of the wild-type inhibitor under the experimental conditions. The results suggest that the R42N mouse SPINK1 variant has a physiologically relevant negative impact on trypsinogen auto-activation.

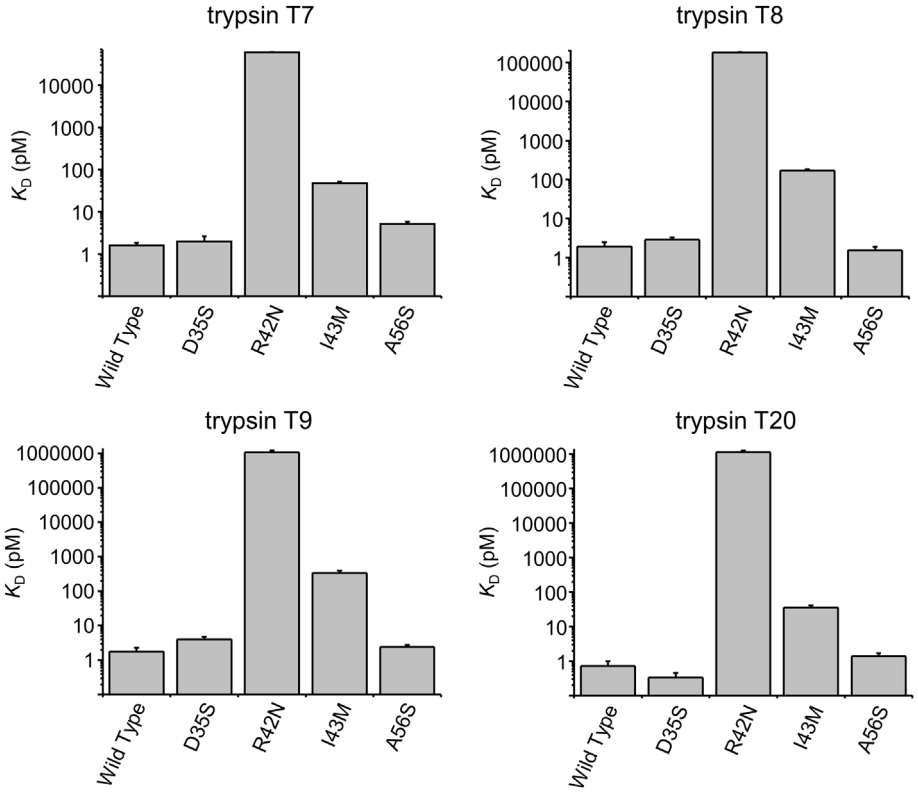

Fig. 5. Inhibition of mouse trypsins by mouse SPINK1 wild type and variants. Binding of SPINK1 to trypsin was characterized by measuring the dissociation equilibrium constant (K_D) values in equilibrium as described in Methods. Data points represent mean ± SD of three experiments.

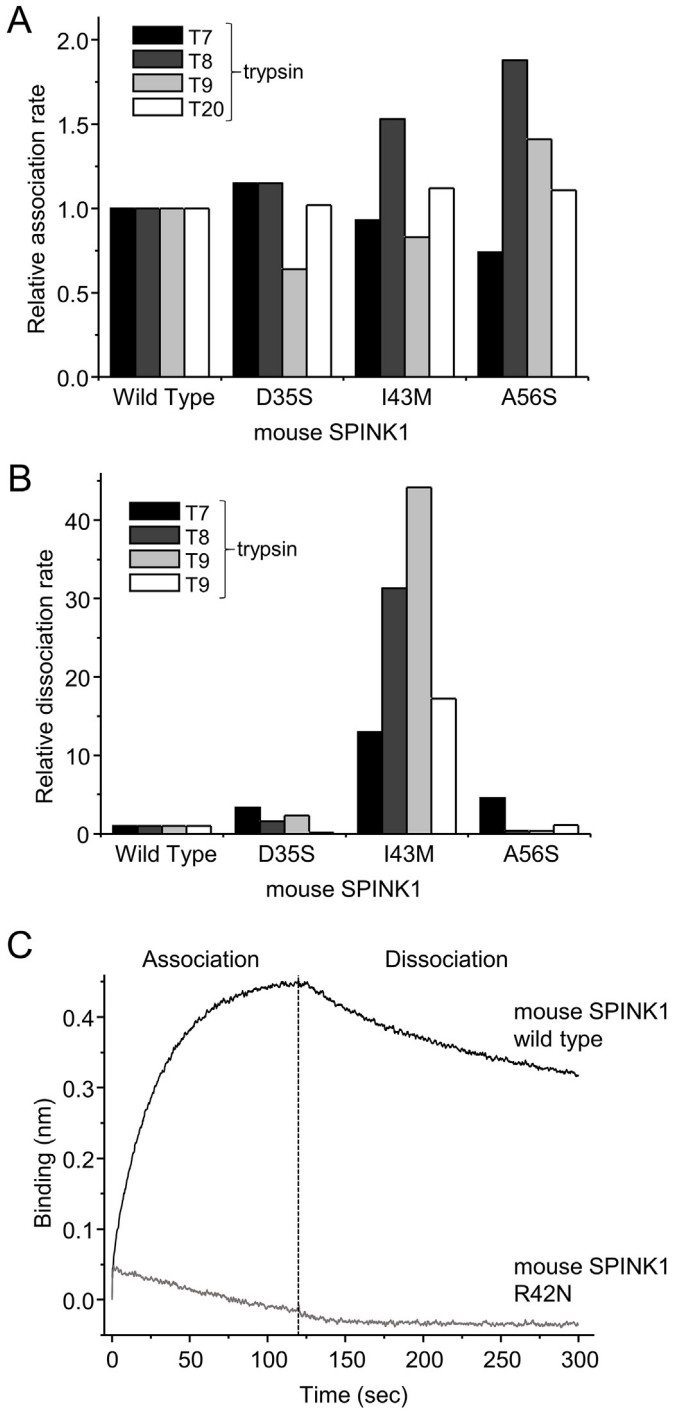

Fig. 6. Binding kinetics of mouse SPINK1 wild type and variants to mouse trypsins. Relative association (A) and dissociation (B) rate constant values are shown. The association and dissociation kinetics of the R42 N variant and wild-type mouse SPINK1 were determined to T7 trypsin with biolayer interferometry (C). Measurements were performed as described in Methods.

Taken together, we demonstrated that mouse SPINK1 is a high affinity inhibitor of mouse trypsins. Functional effects of designated missense SPINK1 mutations identified in chronic pancreatitis were replicable in the experiments with mouse SPINK1. Our results would likely contribute to the development of a genetically engineered SPINK1 mouse model.

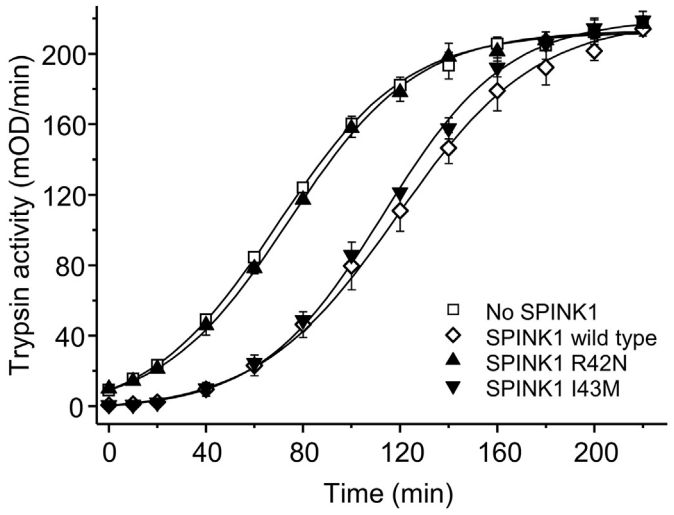

Fig. 7. Effect of mouse SPINK1 wild type and variants on the activation of T7 trypsinogen. Trypsinogen at 1 μM final concentration was incubated with 30 nM initial trypsin in the absence and presence of 40 nM SPINK1 in 0.1 M Tris-HCl (pH 0.8), 1 mM $CaCl_2$ and 0.05% Tween 20 buffer at 37 °C. At indicated time points aliquotes were withdrawn and trypsin activity was measured by the addition of 300 μM final Suc-Ala-Ala-Pro-Lys-p-nitroanilide substrate in the same buffer. Average of three experiments ± SD is shown.

Acknowledgements

This work was supported by the Development and Innovation Office of Hungary grant FK127942 (to AS). The authors are grateful for Ilma Korponay-Szabó and Ádám Diós for help with bio-layer interferometry. Miklós Sahin-Tóth and Mohamed Mahdi are gratefully acknowledged for critical reading of the manuscript and helpful suggestions.

Appendix A. Supplementary data

Supplementary data to this article can be found online at https://doi.org/10.1016/j.pan.2023.04.043.

References

[1] Rinderknecht H, Renner IG, Carmack C. Trypsinogen variants in pancreatic juice of healthy volunteers, chronic alcoholics, and patients with pancreatitis and cancer of the pancreas. Gut 1979;20(10):886–91. https://doi.org/10.1136/gut.20.10.886.

[2] White TT, Allan BJ. Intrapancreatic activation of proteases in the etiology of pancreatitis and cancer of the pancreas. Med Clin 1974;58(6):1305–10. https://doi.org/10.1016/s0025-7125(16)32072-7.

[3] Hegyi E, Sahin-Tóth M. Genetic risk in chronic pancreatitis: the trypsin-dependent pathway. Dig Dis Sci 2017;62(7):1692–701. https://doi.org/10.1007/s10620-017-4601-3.

[4] Ohmuraya M, Hirota M, Araki K, Baba H, Yamamura K. Enhanced trypsin activity in pancreatic acinar cells deficient for serine protease inhibitor kazal type 3. Pancreas 2006;33(1):104–6. https://doi.org/10.1097/01.mpa.0000226889.86322.9b.

[5] Szabó A, Toldi V, Gazda LD, Demcsák A, Tőzser J, Sahin-Tóth M. Defective binding of SPINK1 variants is an uncommon mechanism for impaired trypsin inhibition in chronic pancreatitis. J Biol Chem 2021;296:100343. https://doi.org/10.1016/j.jbc.2021.100343.

[6] Mehner C, Radisky ES. Bad tumors made worse: SPINK1. Front Cell Dev Biol 2019;7:10. https://doi.org/10.3389/fcell.2019.00010.

[7] Geisz A, Sahin-Tóth M. A preclinical model of chronic pancreatitis driven by trypsinogen autoactivation. Nat Commun 2018;9(1):5033. https://doi.org/10.1038/s41467-018-07347-y.

[8] Németh BC, Wartmann T, Halangk W, Sahin-Tóth M. Autoactivation of mouse trypsinogens is regulated by chymotrypsin C via cleavage of the autolysis loop. J Biol Chem 2013;288(33):24049–62. https://doi.org/10.1074/jbc.M113.478800.

[9] Ohmuraya M, Hirota M, Araki M, Mizushima N, Matsui M, Mizumoto T, et al. Autophagic cell death of pancreatic acinar cells in serine protease inhibitor

Kazal type 3-deficient mice. Gastroenterology 2005;129(2):696–705. https://doi.org/10.1016/j.gastro.2005.05.057.
[10] Romac JM, Ohmuraya M, Bittner C, Majeed MF, Vigna SR, Que J, et al. Transgenic expression of pancreatic secretory trypsin inhibitor-1 rescues SPINK3-deficient mice and restores a normal pancreatic phenotype. Am J Physiol Gastrointest Liver Physiol 2010;298(4):G518–24. https://doi.org/10.1152/ajpgi.00431.2009.
[11] Sakata K, Araki K, Nakano H, Nishina T, Komazawa-Sakon S, Murai S, et al. Novel method to rescue a lethal phenotype through integration of target gene onto the X-chromosome. Sci Rep 2016;6:37200. https://doi.org/10.1038/srep37200.
[12] Nathan JD, Romac J, Peng RY, Peyton M, Macdonald RJ, Liddle RA. Transgenic expression of pancreatic secretory trypsin inhibitor-I ameliorates secretagogue-induced pancreatitis in mice. Gastroenterology 2005;128(3):717–27. https://doi.org/10.1053/j.gastro.2004.11.052.
[13] Nathan JD, Romac J, Peng RY, Peyton M, Rockey DC, Liddle RA. Protection against chronic pancreatitis and pancreatic fibrosis in mice overexpressing pancreatic secretory trypsin inhibitor. Pancreas 2010;39(1):e24–30. https://doi.org/10.1097/MPA.0b013e3181bc45e9.
[14] Romac JM, Shahid RA, Choi SS, Karaca GF, Westphalen CB, Wang TC, et al. Pancreatic secretory trypsin inhibitor I reduces the severity of chronic pancreatitis in mice overexpressing interleukin-1beta in the pancreas. Am J Physiol Gastrointest Liver Physiol 2012;302(5):G535–41. https://doi.org/10.1152/ajpgi.00287.2011.
[15] Sun C, Liu M, An W, Mao X, Jiang H, Zou W, et al. Heterozygous Spink1 c.194+2T>C mutant mice spontaneously develop chronic pancreatitis. Gut 2020;69(5):967–8. https://doi.org/10.1136/gutjnl-2019-318790.
[16] Pesei ZG, Jancsó Z, Demcsák A, Németh BC, Vajda S, Sahin-Tóth M. Preclinical testing of dabigatran in trypsin-dependent pancreatitis. JCI Insight 2022;7(21). https://doi.org/10.1172/jci.insight.161145.
[17] Nagel F, Palm GJ, Geist N, McDonnell TCR, Susemihl A, Girbardt B, et al. Structural and biophysical insights into SPINK1 bound to human cationic trypsin. Int J Mol Sci 2022;23(7). https://doi.org/10.3390/ijms23073468.
[18] Boros E, Sebák F, Héja D, Szakács D, Zboray K, Schlosser G, et al. Directed evolution of canonical loops and their swapping between unrelated serine proteinase inhibitors disprove the interscaffolding additivity model. J Mol Biol 2019;431(3):557–75. https://doi.org/10.1016/j.jmb.2018.12.003.
[19] Sahin-Tóth M, Kukor Z, Nemoda Z. Human cationic trypsinogen is sulfated on Tyr154. FEBS J 2006;273(22):5044–50. https://doi.org/10.1111/j.1742-4658.2006.05501.x.
[20] Witt H, Luck W, Hennies HC, Classen M, Kage A, Lass U, et al. Mutations in the gene encoding the serine protease inhibitor, Kazal type 1 are associated with chronic pancreatitis. Nat Genet 2000;25(2):213–6. https://doi.org/10.1038/76088.
[21] Pfutzer RH, Barmada MM, Brunskill AP, Finch R, Hart PS, Neoptolemos J, et al. SPINK1/PSTI polymorphisms act as disease modifiers in familial and idiopathic chronic pancreatitis. Gastroenterology 2000;119(3):615–23. https://doi.org/10.1053/gast.2000.18017.
[22] Kuwata K, Hirota M, Sugita H, Kai M, Hayashi N, Nakamura M, et al. Genetic mutations in exons 3 and 4 of the pancreatic secretory trypsin inhibitor in patients with pancreatitis. J Gastroenterol 2001;36(9):612–8. https://doi.org/10.1007/s005350170045.
[23] Hirota M, Kuwata K, Ohmuraya M, Ogawa M. From acute to chronic pancreatitis: the role of mutations in the pancreatic secretory trypsin inhibitor gene. JOP 2003;4(2):83–8.
[24] Király O, Wartmann T, Sahin-Tóth M. Missense mutations in pancreatic secretory trypsin inhibitor (SPINK1) cause intracellular retention and degradation. Gut 2007;56(10):1433–8. https://doi.org/10.1136/gut.2006.115725.
[25] Boulling A, Le Marechal C, Trouve P, Raguenes O, Chen JM, Férec C. Functional analysis of pancreatitis-associated missense mutations in the pancreatic secretory trypsin inhibitor (SPINK1) gene. Eur J Hum Genet 2007;15(9):936–42. https://doi.org/10.1038/sj.ejhg.5201873.
[26] Masamune A, Kume K, Takagi Y, Kikuta K, Satoh K, Satoh A, et al. N34S mutation in the SPINK1 gene is not associated with alternative splicing. Pancreas 2007;34(4):423–8. https://doi.org/10.1097/mpa.0b013e3180335fd0.
[27] É Kereszturi, Király O, Sahin-Tóth M. Minigene analysis of intronic variants in common SPINK1 haplotypes associated with chronic pancreatitis. Gut 2009;58(4):545–9. https://doi.org/10.1136/gut.2008.164947.
[28] Wu H, Boulling A, Cooper DN, Li ZS, Liao Z, Ferec C, et al. Analysis of the impact of known SPINK1 missense variants on pre-mRNA splicing and/or mRNA stability in a full-length gene assay. Genes 2017;8(10). https://doi.org/10.3390/genes8100263.
[29] Boulling A, Masson E, Zou WB, Paliwal S, Wu H, Issarapu P, et al. Identification of a functional enhancer variant within the chronic pancreatitis-associated SPINK1 c.101A>G (p.Asn34Ser)-containing haplotype. Hum Mutat 2017;38(8):1014–24. https://doi.org/10.1002/humu.23269.
[30] Terlizzi V, De Gregorio F, Sepe A, Amato N, Arduino C, Casale A, et al. Brand new SPINK1 and CFTR mutations in a child with acute recurrent pancreatitis: a case report. Minerva Pediatr 2013;65(6):669–72.
[31] Werlin S, Konikoff FM, Halpern Z, Barkay O, Yerushalmi B, Broide E, et al. Genetic and electrophysiological characteristics of recurrent acute pancreatitis. J Pediatr Gastroenterol Nutr 2015;60(5):675–9. https://doi.org/10.1097/MPG.0000000000000623.
[32] Laskowski M, Wu FC. Temporary inhibition of trypsin. J Biol Chem 1953;204(2):797–805.